EMG Gesture Detection

Elaine Liu, Gabriel Guillen, Kieran Dunn

1. Abstract (Elaine, Gabe, Kieran)

In recent years, the use and popularity of gesture recognition has seen significant growth across health wearables, virtual reality and gaming technology, robotics training, and more. Gesture recognition can be achieved through different means in both software (computer vision and machine learning) and hardware (motion sensors and wearable technology). However, motion sensor and computer vision methods can often be bulky, uncomfortable, and less precise for small movements in the wrists and hands. For more dependable detection of hand movements, we want to further explore the use of electromyography (EMG). EMG—diagnostic tests that measure the electrical activity of muscles—can offer more precise detection of muscles in the hand and wrist. Our project successfully provided an output that was clearly distinct for four American Sign Language gestures. Data signal transmissions were taken using adhesive electrodes that were positioned on the user's forearm, wrist, and hand. These signals were then fed through a network of filters and amplifiers in order to measure the individual muscle responses. The combination of muscle responses showed distinct signals for each ASL gesture.

2. Introduction (Elaine, Gabe, Kieran)

Gesture detection and recognition has numerous applications today and is a very popular area of research. For example, human-computer interaction in virtual and augmented reality environments, as well as gesture-based control of smart home and automotive devices are now major areas of technological development. In assistive devices, gesture recognition can be incredibly useful for people with disabilities, allowing them to interact with smart computer systems. Applications for sign language detection also exist, bridging communication gaps in real time.

Currently, implementations of gesture recognition systems vary widely. Some employ 3D models of hands made of collections of vectors, or even skeletal modals, to provide computer algorithms with positional information for gesture inference. Other approaches use "appearance-based algorithms," which form 2D representations of the input and use large visual datasets of hands to find the closest matches of gestures. Numerous challenges—including variability in image quality, poor lighting, and different camera specs—exist in both of these cases. Furthermore, developing and running a general algorithm to cover such a broad range of scenarios is not only incredibly difficult but also computationally expensive.

Electromyography (EMG) is another method to achieve gesture recognition that avoids many of the aforementioned issues by looking at specific muscles. EMG measures electrical activity in response to nerve stimulation of muscles between electrodes. As muscles contract more strongly, more muscle fibers activate and produce action potentials. Between surface and invasive EMG, we will explore the use of surface EMG to evaluate muscle activity and differentiate between hand gestures based on the individual muscles activated.

The ASL alphabet was chosen as the set of gestures we would pull from due to its high practicality for communication, large amounts of documentation, and the range of motions being generally wrist and above, meaning we could constrain our electrode placement to the elbow and above.

3. Design

Block Diagram (Kieran)
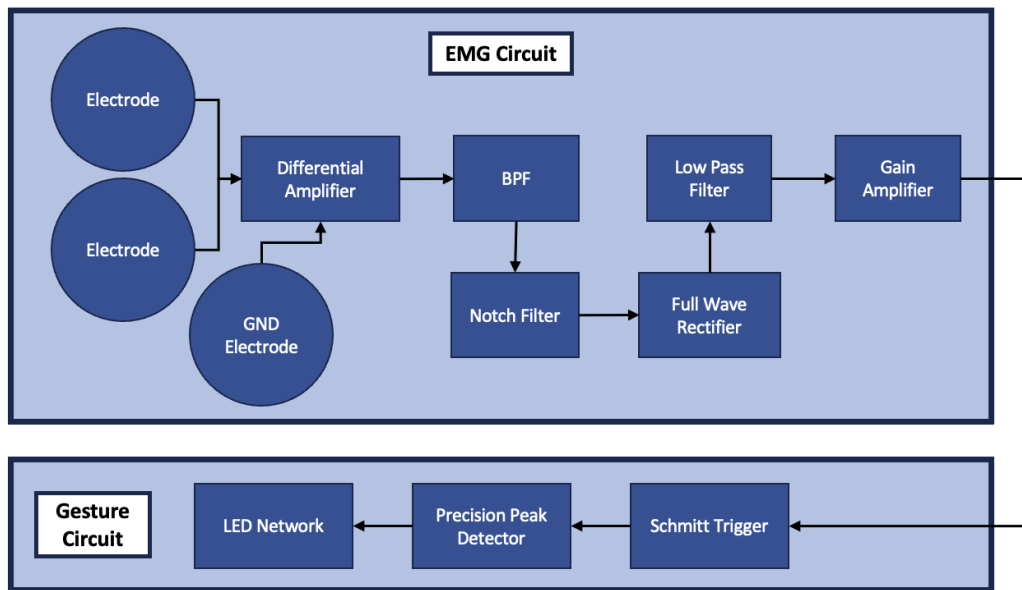
Our circuit at a very high level consists of 3 individual EMG detection circuits which are used to measure the electrical activity of distinct muscles. Then, these signals are fed through our gesture detector circuit, which will take in each signal, activate a certain LED based on the output level of the signal, and the combination of LEDs that are activated will allow us to see which gesture was performed.

3.1: EMG Detection Circuit (Kieran)

The first subset of our system is the EMG detection system, which uses three electrodes to measure a muscle's electrical activity. The first two electrodes are placed across a muscle while the ground electrode is placed in a part of the body with low muscle density such as the elbow. This allows us to read the difference in electrical action potential at each electrode as it travels down the contracting muscle while removing motion artifact noise or other sources of noise. This is fed into the EMG, which removes low and high frequency noise to isolate the primary energy of the muscles electrical activity and then performs envelope detection to smooth out the signal's high frequency fluctuations into a general trend of its amplitude over time.

### 3.1.1: Differential Amplifier (Kieran)
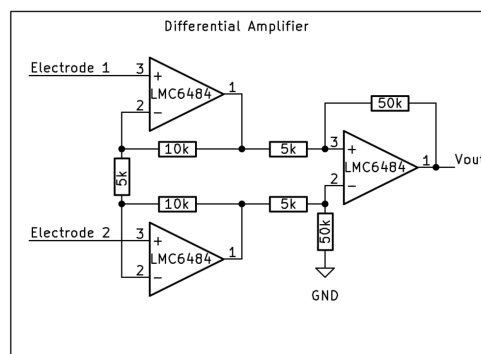
The differential amplifier is the first circuit block that the raw electrical muscle signal is sent through. Thus, the goal of the differential amplifier is to remove excess noise such as movement artifacts, electrical signals from the cables, or any other signal that affects both electrodes. This is done using an op-amp based differential amplifier where the operation amplifiers utilized were LMC6484. These were chosen for their low crossover distortion and ability to amplify very low amplitude, high frequency signals, allowing the raw EMG signal to be sent into the circuit with minimal distortion or artifacts. The next goal of the operational amplifier was to amplify the signal so it could be more easily manipulated and utilized in later stages. The amplification was done using the equation $(1 + \frac{10k+10k}{5k}) \times \frac{50k}{5k} \approx 50$.
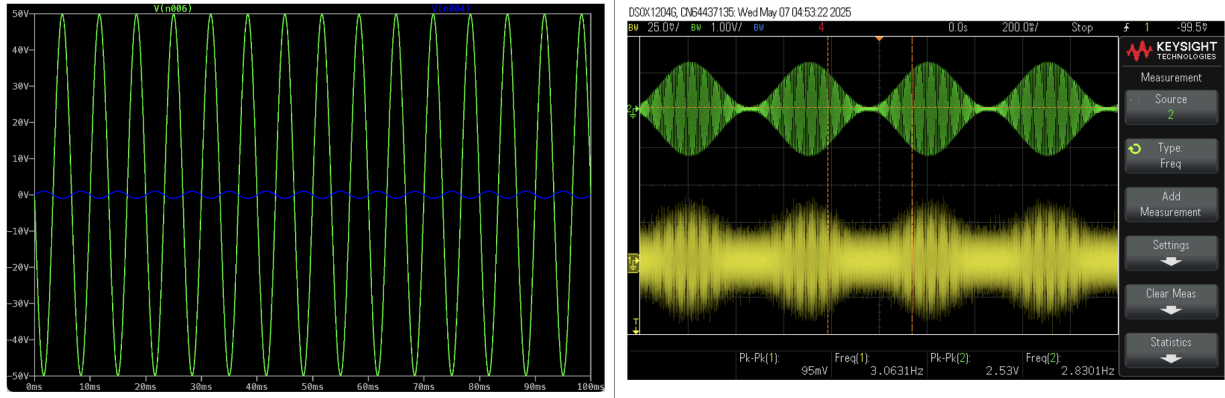

The performance of the operational amplifier can be seen in the picture above. The picture on the right shows the yellow input signal and green output signal, where there is a gain of 26.63. This is less than the gain shown in the simulated performance, but this decrease in performance could be due to the challenges around viewing sub 100mV signals on the oscilloscope as well as the lack of exact resistors available in the lab. The simulated performance shown in the photo on the left displays the input sine wave in blue (the other input to the differential amplifier is sent to ground) and the output in green, and a clear gain of 50 can be seen.

3.1.2: Bandpass Filter (Kieran)
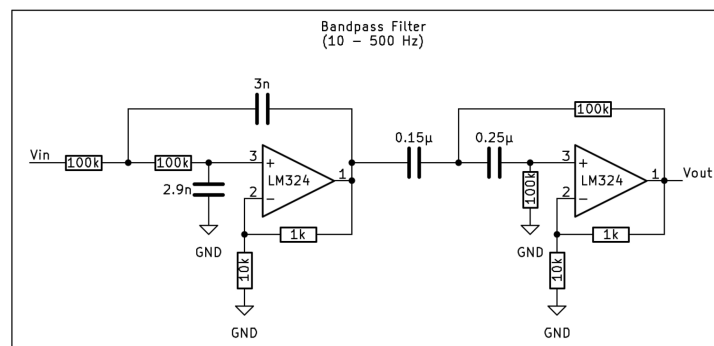
The bandpass filter is used to isolate signals only related to muscle signals. This is another stage that removes low frequency and high frequency noise that might not be common to both electrodes but still unrelated to muscle activity. Most muscle activity is within the 10 to 500 Hz range, so the configuration of the bandpass is a Sallen-Key Low Pass filter removing above 500 Hz and a Sallen-Key High Pass filter to remove sub 10 Hz signals. Both filters utilize equations of $\frac{1}{\sqrt{2*\pi*R_1*R_2*C_1*C_2}}$ within the path of the

non-inverting input. The gain of the amplifier is in the inverting input using the equation $1 + \frac{1k}{10k}$ which is approximately 1.
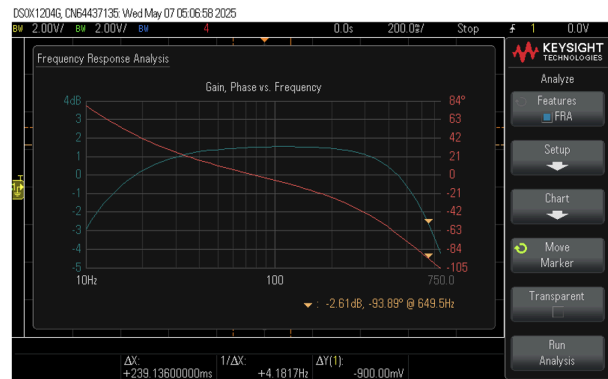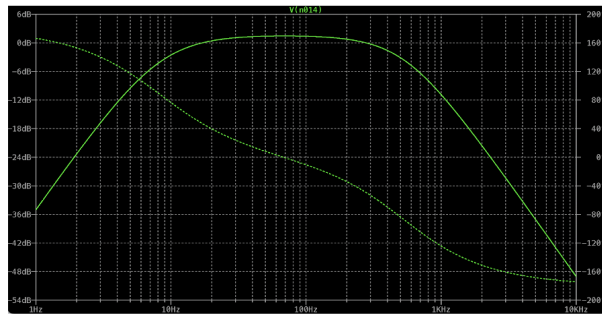

The simulated performance on the left is very similar to the actual performance on the right with both graphs having -3 dB points around 10 Hz and 500 Hz with slight variations in the exact filtered frequencies, which could be due to challenges related to inductance within breadboard rails or capacitance from component leads. Both also have a very low gain, which is to be expected.

### 3.1.3: Active Twin-T Notch Filter (Gabriel)
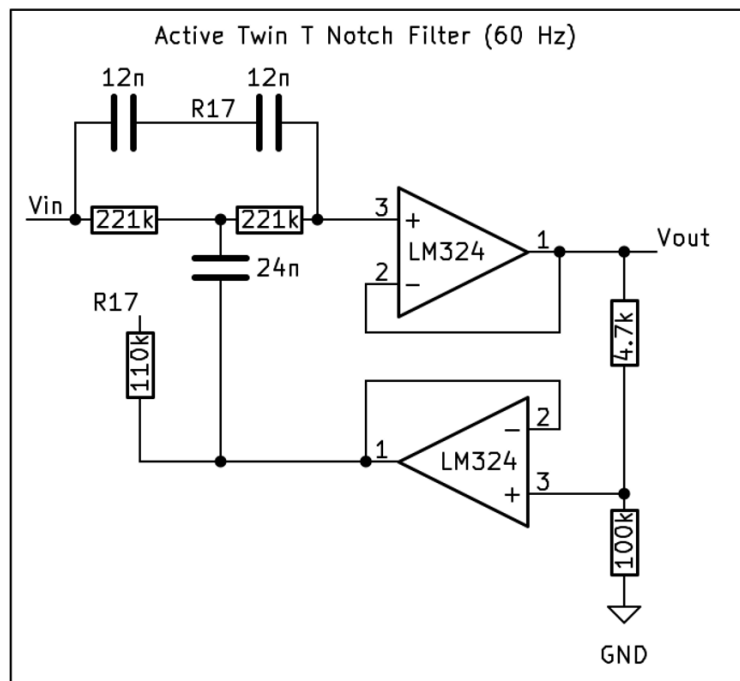
The purpose of the active twin-t notch filter is to eliminate the 60Hz signal broadcast from the Prudential Tower. Given that the EMG signal input can be on the order of millivolts to microvolts, even a small 60Hz signal from Prudential could have a large impact, especially given the high amounts of gain in later stages. The decision to use an active twin-t notch filter was made due to the fact that, when analyzing the frequency response, other notch filter designs had much lower magnitude slopes around the 60Hz frequency, causing higher attenuation over a much wider range. This would have compromised our project given that EMG signals can range from 1Hz to 500Hz, and attenuating out too much of this range

risks weakening our desired EMG signal. Thus, the active twin-t notch filter was selected due to its higher magnitude slopes around 60Hz, making it so that the -3dB points were within 5Hz on either side, isolating the 60Hz signal we wanted to eliminate, and minimizing the impact on our signal.
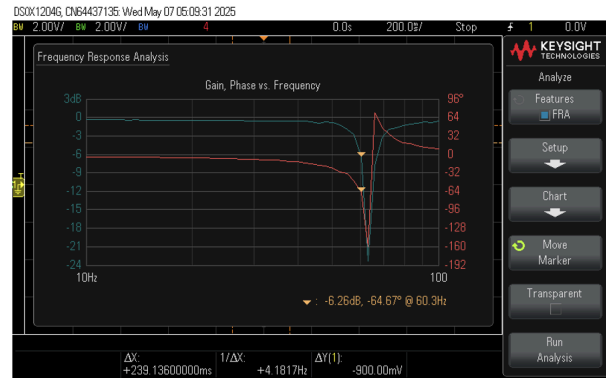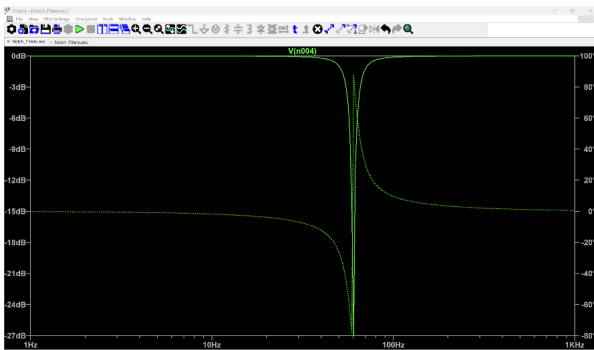

Comparing the simulation of this notch filter (left image) to the physical implementation (right image), we can see a difference in the center frequency, with the physical implementation's center frequency about 3-4 Hz higher than expected. This is mainly due to the fact that values of components needed to achieve a center frequency of exactly 60 Hz were very specific and required us to combine multiple components in series or parallel to achieve such values. This is most predictably the source of imprecision in the filter. However, this discrepancy did not impact the performance heavily, as an attenuation of -6.26 dB was still achieved for 60 Hz signals. Furthermore, the magnitude of the slopes in the bode plot were unchanged, keeping the -3dB points within 5 Hz of the center frequency, minimizing the risk of attenuating our EMG signal.

3.1.4: Precision Full Wave Rectifier (Gabriel)
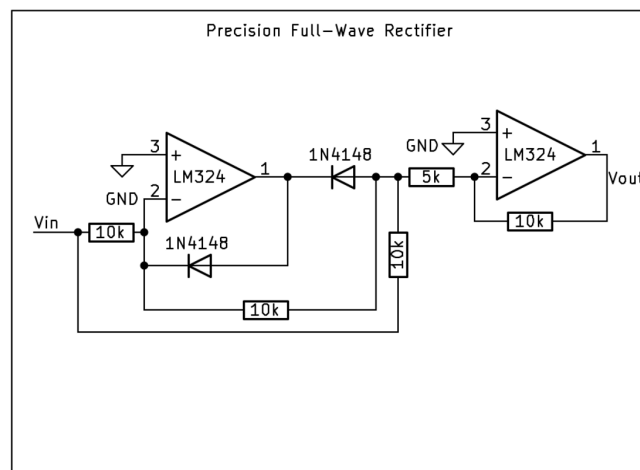
The purpose of the precision full wave rectifier is to bring the EMG signal to be fully positive. EMG signals are inherently both positive and negative, but both polarities carry important information about the muscle contraction, with voltage magnitude being highly correlated to strength of contraction. Thus bringing the EMG signal to be fully positive allows for easy analysis of the muscle's contraction strength through voltage peak detection. The decision to use a precision full wave rectifier design over other

rectifying designs was due to the fact many non-precision designs have an output 0.6V to 0.7V lower than the input, which was unacceptable in our project due to the low voltage magnitude and high precision of EMG signals. Thus, the precision full wave rectifier was a perfect fit due to the voltage magnitude drop across it being negligibly small, maintaining our EMG signal. As shown below, there is no significant difference between the simulated results (left) and the results from the physical implementation (right).
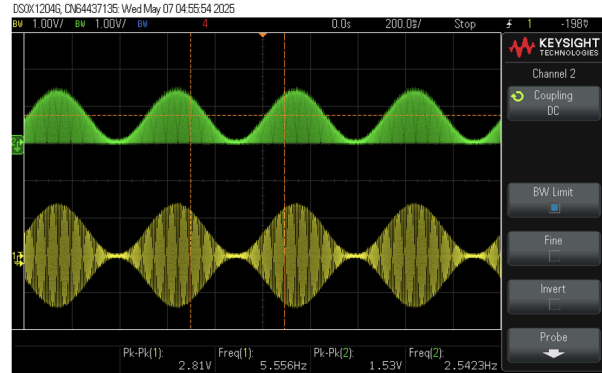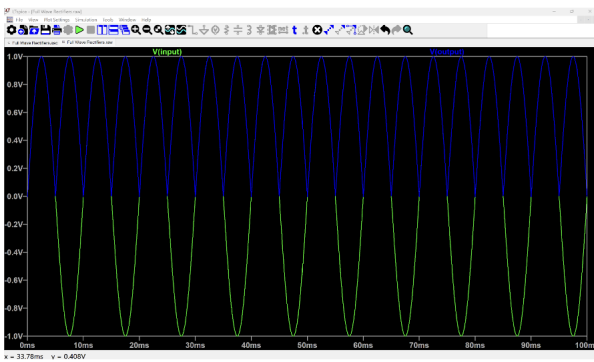

3.1.5: Low Pass Filter (Elaine)

A low pass filter is required at this stage to capture the lower frequency of the rectified signal and create an envelope of the EMG—these will give the desired information about overall muscle movement, as it extracts overall amplitude changes in the signal over time rather than particular frequencies of a muscle contraction. To effectively remove higher frequencies without introducing distortion, a second order Sallen-Key low pass filter is used, built with a LM324 operational amplifier. Values for the resistors and capacitors were calculated based on a desired filtering above 3.6Hz, a common frequency of muscle EMG amplitude changes over time, with the equation $3.6Hz = \frac{1}{(2\pi \times \sqrt{R_1 R_2 C_1 C_2})}$.

Setting C_1 and C_2 to 1µF and ensuring that R_1 and R_2 closely fulfilled Butterworth response constraints ($R_2 = 2R_1$) for a smooth, uniform response in the passband, values of 20k and 39k were used. (In testing, it was found that 39k better achieved a filter above 3.6Hz as compared to a 40k resistor).
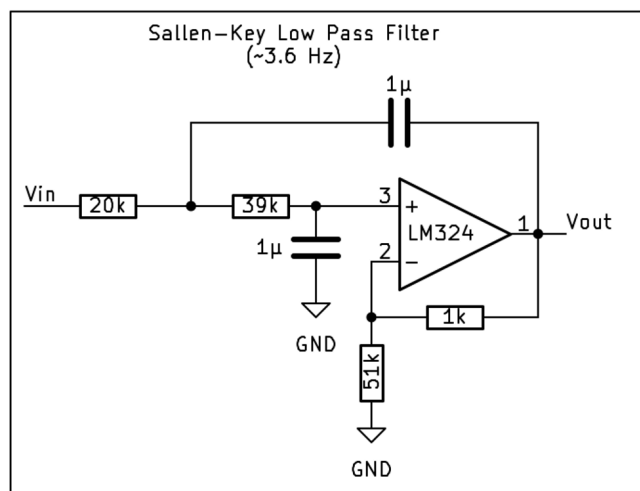

The filter ultimately worked as expected. While the expected behavior cannot be seen on the scope, as it has a minimum frequency of 10Hz, a -3dB point of approximately 3.591Hz was observed on LTSpice.
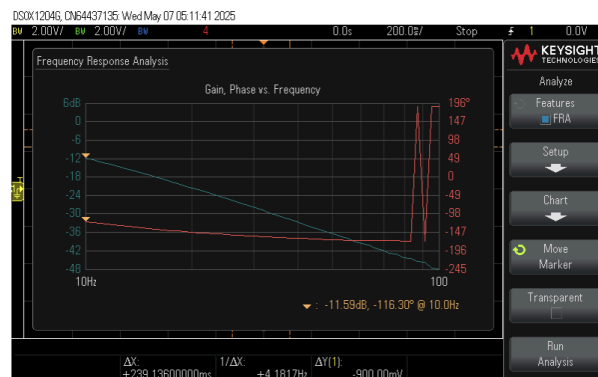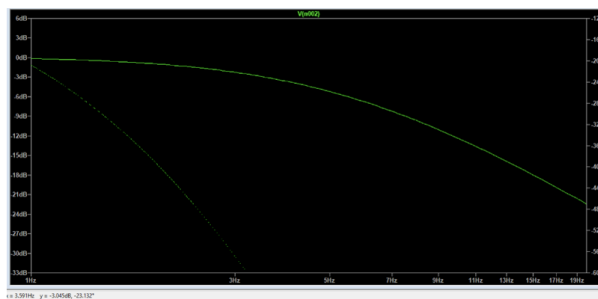
3.1.6: Gain Amplifier (Elaine)

Finally, a non-inverting amplifier was used to achieve signal voltage values large enough for detection use. For flexibility—and to adjust toward whichever gain value best achieved those values—this gain amplifier was initially designed with a 100kΩ potentiometer resistor in series with the 1kΩ resistor. Ultimately, a gain of 100 was tested and found to be effective for the last stage of the EMG circuit, so the circuit simplified to the schematic below. The values were calculated using the equation

$$gain \; = \; \frac{V_{out}}{V_{in}} \; = \; \frac{R_2}{R_1} + 1.$$
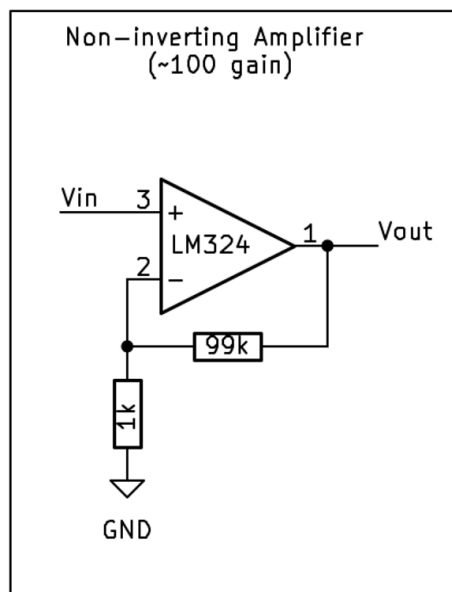
The amplifier was built with an LM324 operational amplifier and worked as expected in the final version of the circuit. The oscilloscope image below shows the gain amplifier with the potentiometer resistor (adjusted for a smaller gain) still included in the schematic for visual effect and clarity, so that both input and output signals could be clearly seen. In the final version, the gain observed more closely followed the LTSpice image below with a gain of ~40dB, or 100.
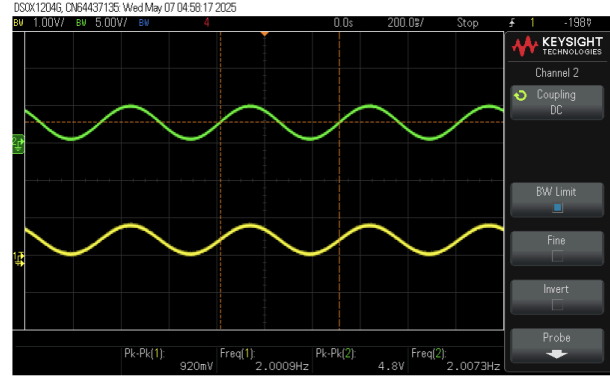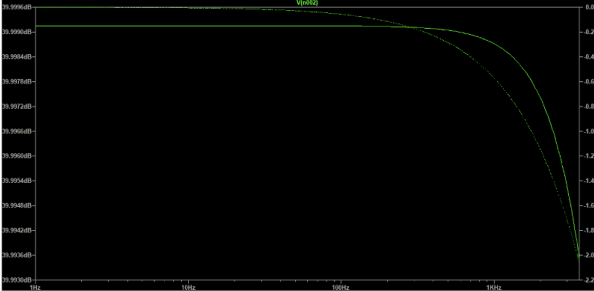
3.2: Gesture Circuit (Gabriel)

The second subset of our system is our gesture circuit, which consists of a Schmitt trigger, peak detector, and LED network, allowing us to analyze the magnitude of the muscle contraction, set hysteresis bounds dictating what magnitude corresponds to a gesture, and output a sustained voltage to light up the LED corresponding to the correct muscle group. This subsystem is unique for each signal path, given that the hysteresis bounds for each muscle group vary.

3.2.1: Schmitt Trigger (Elaine)

A schmitt trigger was implemented for each EMG circuit to digitally identify when the user performs a gesture. After testing the EMG circuits on various muscle groups, the following thresholds were observed for when a signal reflected an active gesture:

|	Low threshold, right above voltage at resting position	High threshold, right under peak voltage upon gesture
Muscles involved in moving the thumb down and wrist down independently	2V	3V
Muscles involved in closing a fist	2V	2.5V

For both muscle groups, the following equation was used:

$$V_{bias} = \frac{V_{threshold, low} + V_{threshold, high}}{2}$$

$V_{in} = V_{out} \times \frac{R_1}{R_2}$, where V_{in} is $\frac{V_{threshold, low} - V_{threshold, high}}{2}$ and V_{out} is the saturation voltage.

As the operational amplifiers were powered with a $\pm 7V$ supply line, V_{out} was 7V. Thus, for the muscles involved in moving the thumb and wrist down, the equation became $\frac{3V-2V}{2} = 0.5V = 7V \times \frac{R_1}{R_2}$, and for the muscles involved in closing a fist, $\frac{2.5V-2V}{2} = 0.25V = 7V \times \frac{R_1}{R_2}$. With R_1 set as 1kΩ for each circuit, R_2 was found thereafter.
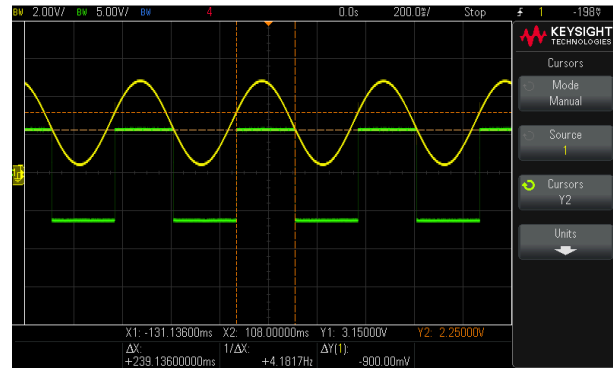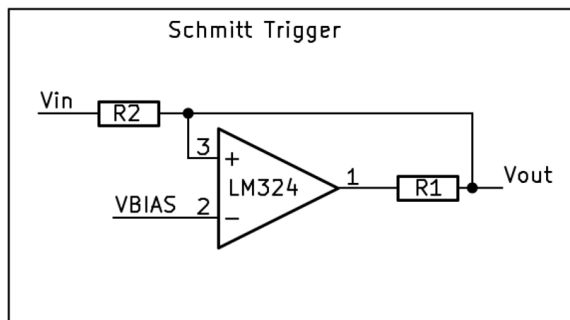

The schmitt triggers were built with LM324 operational amplifiers and worked closely as expected—when tested with a wave function generator, high thresholds of 3.15V and low thresholds of 2.25V were observed. While they were a little off from initial calculation expectations, these thresholds were sufficient for real life gesture detection and were kept.

3.2.2: Peak Detector (Kieran)
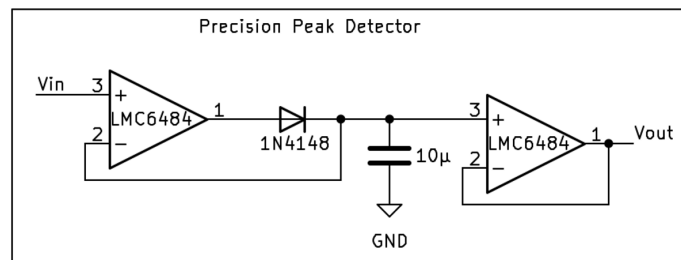
The precision peak detector is used to ensure that the highest voltage peak stays elevated for enough time so that it can be viewed on the LED. This was created using two LMC6484 operational amplifiers for their higher speed when compared to LM324 op amps. The circuit uses the decay equation based on the discharge current from the capacitor divided by its capacitance, so the primary component we could change was the capacitor. 10 µF was used primarily because it gave us a slow enough decay to keep the LED elevated for a necessary but not too long amount of time. Larger capacitors could have been used but would ultimately lead to a longer elevated voltage signal, which was not necessary.
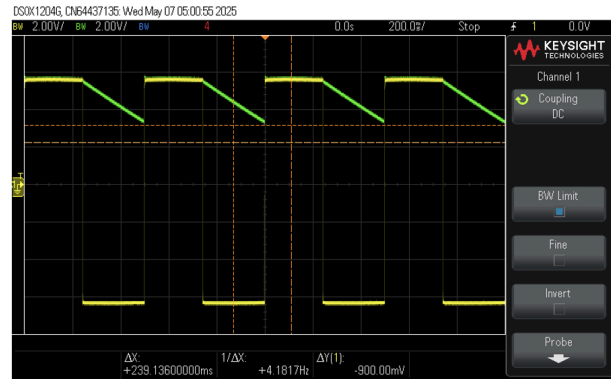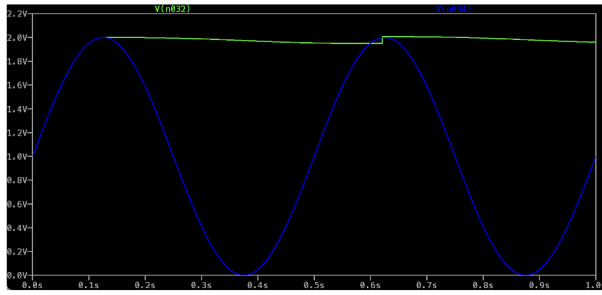
The simulated performance of the circuit is shown in the picture on the left while the actual performance is shown in the picture on the right. The output signal in both is represented in green. It is challenging to measure the performance of the peak detector circuit, but it is fairly good in both cases at tracking the input voltage and ensuring that it stays elevated, which was all that was necessary for our purposes.

3.2.3: LED Network (Gabriel)

To fully display our output, we connected the output of each peak detector to a LED with a unique color. Given our project used 3 signal paths, we had 3 LED's total (red, blue, green), and this corresponds to us having 3 bits of information at our output. The LED turning on displays a contraction for that muscle group, and thus our 8 possible states correspond to different pairings of muscle contractions, with 7 possible states for gestures, and 1 state for a neutral pose. Through this, the LED network output is just a code directly corresponding to a specific state/gesture.

The final comprehensive circuit can be seen in the image below, with the LED's at the top breadboard.
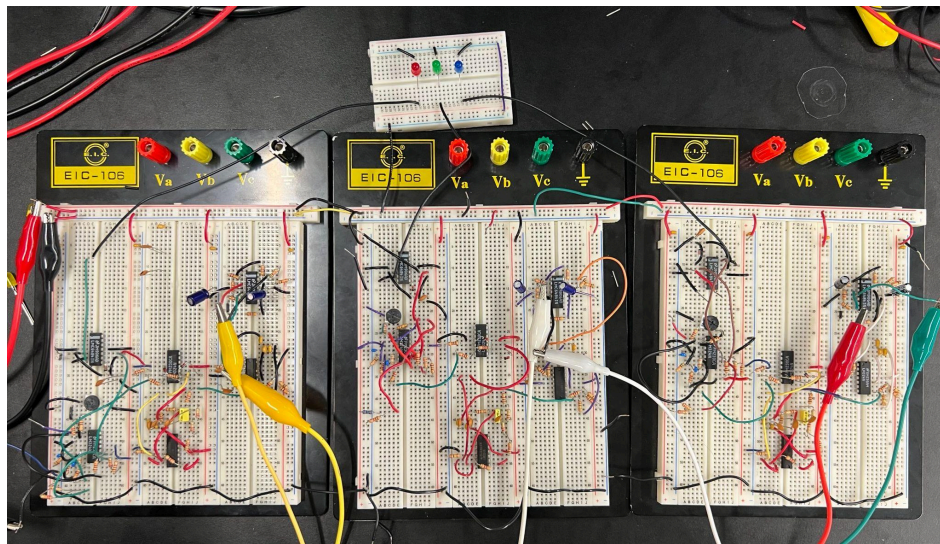
3.3: Electrode Placement (Elaine)

To best identify the muscles involved in various ASL gestures, different muscle groups were researched and tested. The following muscle groups showed most notable results for producing prominent signals of around 3V+ at gesture peak: the abductor pollicis brevis and flexor pollicis longus for the muscles involved in moving the thumb, the flexor digitorum superficialis and flexor digitorum profundus involved in closing the fist, and the flexor carpi radialis involved in turning the wrist downward. Below is an image of Gabriel's arm with electrode placements at the respective muscle groups, with an electrode at the elbow for a ground reference point. There is also an attached scientific diagram of forearm muscles for reference.
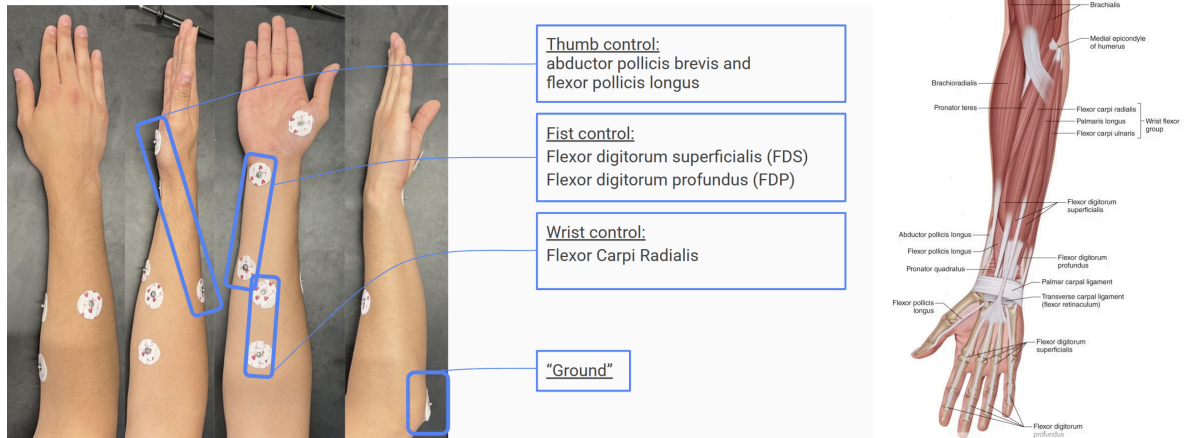

4. Results

4.1: Discussion (Elaine)

Ultimately, the circuit, as shown below, worked quite well on the aforementioned muscle groups. Peak signals of at least 2.5V for a closing fist gesture and 3V for wrist down and thumb gestures were output, as shown in the table across five trials below.

	Min Voltage (V)	Max Voltage (V)
Flexor Carpi Radialis, Wrist Down	1.75	3.22
	1.83	4.5
	1.93	3.78
	1.83	4.02
	1.83	3.78
Flexor Digitorum Superficialis and Flexor Digitorum Profundus, Closed Fist	1.83	3.26
	1.83	3.5
	1.83	3.34
	1.83	2.66
	1.83	3.16

Combining those muscle group gestures, larger ASL gestures were able to be detected. The ASL A, B, M, and Q letters were some of the most clearly identifiable gestures, with a lit up LED in response for each muscle involved as a "bit" of information. Gabe can be found performing each gesture in the image below, with the respective LED's shown lighting up. The gestures were detected consistently for deliberate hand movements engaging the aforementioned muscles at an even speed. There were, however, inconsistencies if the gestures were too fast, relaxed, or varying in angle. As such, the reliability of this system depended on the consistency of the user's gestures.
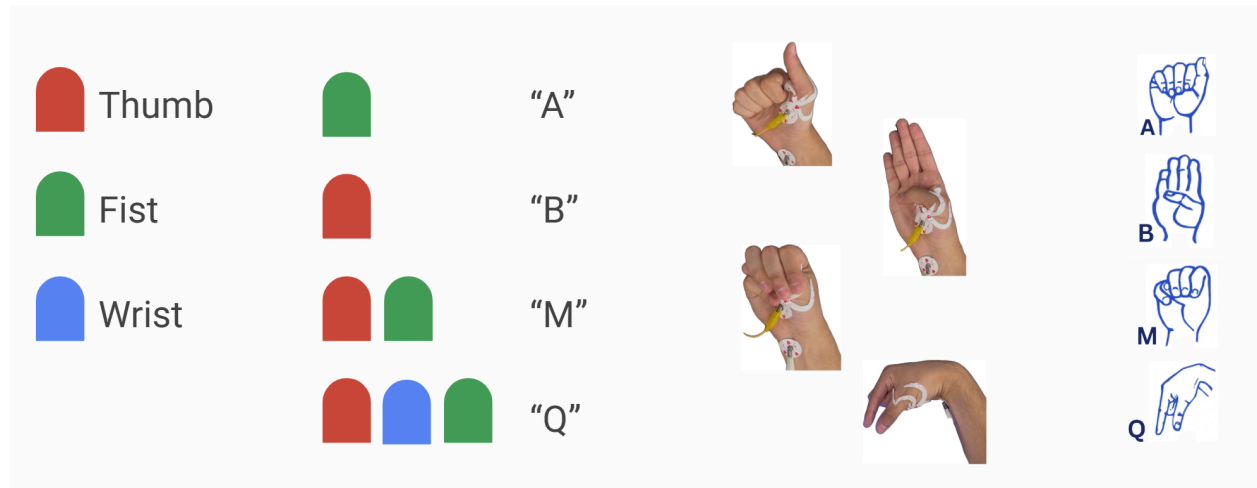
4.1: Future Iterations/improvements (Gabe)

One main area for improvement is in the level of signal processing done on each signal path. During the course of our project, we had to decide whether to choose one muscle group and do very precise analysis of that signal path, or whether to proceed with multiple muscle groups and focus on a signal aspect of each signal path. Given that we chose the second, the first would be a very beneficial improvement to this project as we could dive deeper into each signal and not just focus on the magnitude, but also other factors such as duration and speed. This would increase the number of bits of information we can extract from each signal path, thus greatly increasing our total number of gestures we can detect.

Another area for improvement would be in the overall robustness of our circuit. During our testing to find the average DC voltage of each muscle group along with its peak output upon contraction, we found that even when analyzing the same muscle group between the three of us on this team, everyone had a different DC voltage along with peak voltage capability. This meant that for the purposes of setting the hysteresis bounds for the Schmitt trigger, they had to be specific to only one person, limiting the ability for this system to be immediately applied to anyone else. Implementing another subcircuit to help eliminate differences in DC bias would help greatly bring every person's results into a more similar range, improving overall robustness as the Schmitt trigger hysteresis bounds would not need to be adjusted so much.

5. Conclusion (Kieran)

The initial goal of this project was to demonstrate the use of electromyography as a viable alternative to computer vision or machine learning based gesture detection approaches. We were able to show the successful detection of four different American Sign Language hand gestures as well as a clear signal displaying the contraction of three different muscles. Given the time frame of the project as well as the limited component availability, this was a great success, and we hope that it has demonstrated the immense potential of analog-based gesture detection.